

Optimal crop canopy architecture to maximise canopy photosynthetic CO₂ uptake under elevated CO₂ – a theoretical study using a mechanistic model of canopy photosynthesis

Qingfeng Song^{A,B}, Guilian Zhang^{A,B} and Xin-Guang Zhu^{A,B,C}

^ACAS Key Laboratory of Computational Biology and CAS-MPG Partner Institute for Computational Biology, Shanghai Institutes for Biological Sciences, Chinese Academy of Sciences, Shanghai, 200031, China.

^BState Key Laboratory of Hybrid Rice, CAS-MPG Partner Institute for Computational Biology, Shanghai Institutes for Biological Sciences, Chinese Academy of Sciences, Shanghai, 200031, China.

^CCorresponding author. Email: zhuxinguang@picb.ac.cn

Abstract. Canopy architecture has been a major target in crop breeding for improved yields. Whether crop architectures in current elite crop cultivars can be modified for increased canopy CO₂ uptake rate (A_c) under elevated atmospheric CO₂ concentrations (C_a) is currently unknown. To study this question, we developed a new model of canopy photosynthesis, which includes three components: (i) a canopy architectural model; (ii) a forward ray tracing algorithm; and (iii) a steady-state biochemical model of C₃ photosynthesis. With this model, we demonstrated that the A_c estimated from ‘average’ canopy light conditions is ~25% higher than that from light conditions at individual points in the canopy. We also evaluated theoretically the influence of canopy architectural on A_c under current and future C_a in rice. Simulation results suggest that to gain an optimal A_c for the examined rice cultivar, the stem height, leaf width and leaf angles can be manipulated to enhance canopy photosynthesis. This model provides a framework for designing ideal crop architectures to gain optimal A_c under future changing climate conditions. A close linkage between canopy photosynthesis modelling and canopy photosynthesis measurements is required to fully realise the potential of such modelling approaches in guiding crop improvements.

Additional keywords: canopy architecture, elevated CO₂, photosynthesis, ray tracing, sunlit–shaded model.

Received 22 February 2012, accepted 26 November 2012, published online 22 January 2013

Introduction

Improving photosynthetic capacity is one of the main approaches to further enhance crop productivity (Long *et al.* 2006b; Zhu *et al.* 2010), since canopy rather than leaf photosynthesis is closely related to crop yields. One of the major mechanisms underlying the improved crop yields during the ‘green revolution’ has been improved canopy architectures. In particular, selection of cultivars with more erect leaves, especially at the top of the canopy, has led to improved light environments inside a canopy and hence, improved canopy photosynthetic CO₂ uptake rate (A_c) (Long *et al.* 2006b). Though there is still some controversy regarding whether improving photosynthesis can lead to increased crop yields, this may be more related to using leaf rather than canopy photosynthesis in deriving the relationship (Zelitch 1982). The challenge now is how to identify the ideal canopy architectural and leaf metabolic features to breed or engineer for increased canopy photosynthesis for current, and more importantly, for future elevated CO₂ conditions. This is a challenge, partially due to the lack of efficient methods to measure A_c , although many efforts have been devoted to developing canopy photosynthesis chambers (Reicosky and Peters 1977; Steduto *et al.* 2002). Given the logistic difficulty of estimating

canopy photosynthesis in the field, mathematical modelling has typically been used to estimate A_c .

Many canopy photosynthesis models with different levels of details have been developed to date. Depending on the level of complexity, these models can be roughly divided into three categories: (i) the big-leaf model (Running and Coughlan 1988; Thornley and Johnson 1990; Sellers *et al.* 1992; Amthor 1994; Kull and Jarvis 1995; Lloyd *et al.* 1995); (ii) the sunlit–shaded model (de Pury and Farquhar 1997; Wang and Leuning 1998; Dai *et al.* 2004); (iii) and the multi-layer model (deWit 1965; Duncan *et al.* 1967; Lemon *et al.* 1971; Norman 1979). The big-leaf model assumes that the leaf nitrogen is optimally distributed to match the light environments inside a canopy (Sellers *et al.* 1992; Amthor 1994; Lloyd *et al.* 1995). Farquhar (Farquhar 1989) demonstrated that equations describing leaf photosynthesis are the same as those for chloroplast photosynthesis as long as (a) the chloroplast photosynthetic capacity is proportional to the irradiance it absorbs; and (b) the responses of the photosynthetic CO₂ uptake to irradiance are identical among different chloroplasts. This principle was extended to the canopy and formed the basis for the big-leaf canopy photosynthesis models. However, inside a canopy, the light distribution is highly

heterogeneous both spatially and temporarily, mostly due to the heterogeneity of leaf angles and the sunflecks deep in the canopy (de Pury and Farquhar 1997). Such heterogeneities are ignored in current big-leaf, sunlit–shaded and multilayer models. Given this inaccuracy, some model parameters – namely the photosynthetic capacity (Lloyd *et al.* 1995) and the smoothness of the transition from light-limited to light-saturated photosynthesis (Sellers *et al.* 1992; Amthor 1994), i.e. the curvature factor – can be adjusted in the big leaf model. This improves the prediction accuracy of the big-leaf models; however, it renders big-leaf models essentially unscaleable in the sense that these parameters, e.g. curvature factors, need to be modified dependent on the leaf area index (LAI), leaf nitrogen content and the proportion of diffuse light (de Pury and Farquhar 1997). This also makes direct interpretation of the parameters used in the big-leaf model very difficult.

The other extreme of the canopy photosynthesis model is the multi-layer model, where the whole canopy is divided into many categories of leaves, each with different light levels. Most of these models are based on two assumptions: (i) that radiation attenuation inside canopy can be predicted by Beer's Law (Monsi and Saeki 2005); and (ii) that the light inside a canopy can be divided into two categories, i.e. direct and diffuse light, dependent on the different attenuation in canopies (Goudriaan 1977). In these models the predicted light environment for each leaf category is combined with leaf photosynthesis models to predict A_c . These multi-layer models have the flexibility of incorporating the heterogeneity in both environmental and physiological parameters. So far, these models are considered as the most accurate canopy photosynthesis models, with the major drawback of being complex and requiring longer computation time.

The intermediate class of models are the sunlit–shade canopy photosynthesis models. The sunlit–shaded canopy photosynthesis model simplifies the multi-layer model by dividing the whole canopy into two categories of leaves: (i) sunlit; and (ii) shaded leaves (Sinclair *et al.* 1976; Norman 1980). The key for the prediction accuracy relies on the capacity to predict (a) the proportion of the sunlit leaf area and shaded leaf area; and (b) the light levels in the sunlit and shaded leaves. Modelling comparison has demonstrated that the sunlit–shaded model predicted similar A_c as the multi-layer canopy models (de Pury and Farquhar 1997). Besides sunlit–shaded models, another approach to simplify the multi-layer model is to derive analytical solutions of canopy photosynthesis (Acock *et al.* 1978; Johnson and Thornley 1984). However, the predictions using this approach are not as accurate as the sunlit–shaded models (Boote and Loomis 1991).

The sunlit–shaded model has been used in various applications. First, it has been used to identify options to engineer for higher canopy CO₂ uptake rates (Zhu *et al.* 2004a; Ort *et al.* 2011). It has also been extended to include the interaction of stomatal conductance and photosynthesis and even the response of stomatal conductance to water vapour deficit and soil water content, which enabled prediction of net photosynthesis, latent and sensible heat flux of a canopy under a wide range of soil water availability and meteorological conditions (Wang and Leuning 1998). The sunlit–shaded model was also applied in forest studies, for example, to

calculate the forest primary production (Kotchenova *et al.* 2004), CO₂ uptake (Catovsky *et al.* 2002) and the effect of urban forest on air pollutant dry deposition (Hirabayashi *et al.* 2011). Recently, it was used to model the growth and production of the bioenergy crop *Miscanthus × giganteus* (Miguez *et al.* 2009). The sunlit–shaded canopy photosynthesis model was also used as a major tool in the agro-ecology, e.g. in the study of canopy transpiration (Tuzet *et al.* 2003; Yang *et al.* 2009; Chen *et al.* 2011) and evapotranspiration of winter wheat (Mo and Liu 2001), effect of elevated CO₂ on plant (Reynolds *et al.* 1992) and the effects of clouds and atmospheric particles on plant (Roderick *et al.* 2001; Gu *et al.* 2002).

However, all these above-mentioned models are unable to predict the precise light environment inside a canopy with defined canopy architecture and therefore, cannot precisely predict the spatial and temporal heterogeneities of light inside a canopy. However, such heterogeneities of the light environment is extremely important to gain an accurate prediction of A_c , ignoring this heterogeneity can lead to an overestimate of A_c for a canopy (Zhu *et al.* 2012). As a result, the current used sunlit–shaded canopy photosynthesis model cannot predict the influence of modifying canopy architecture, such as tiller number, leaf shape or leaf angle on A_c . With regards to this, a few models representing 3D canopy architectures for different crops including maize (España *et al.* 1999; Guo *et al.* 2006; Zheng *et al.* 2008), rice (Watanabe *et al.* 2005; Zheng *et al.* 2008) and wheat (Evers *et al.* 2007) have been developed in recent years.

This paper describes a model of canopy photosynthesis in which the canopy architecture and light environment inside a canopy is simulated in detail: these two components are then combined with the steady-state biochemical model of C₃ photosynthesis (Farquhar *et al.* 1980) to predict A_c . With this model, we studied the influence of canopy architecture on canopy photosynthesis and explored the theoretical impact of elevated CO₂ on optimal canopy architectures required to maximise A_c .

Materials and methods

Construction of a 3D canopy architecture model

In this study, we used the architectural features of the indica rice Teqing (*Oryza sativa* L. subsp. *indica*). The cv Teqing was planted in Beijing (39.92°N and 116.46°E) on 1 June (day 150) in 2009. To define the plant structure, several parameters were measured, including tiller number, leaf number, leaf base height, leaf length, leaf width, leaf angle and leaf curvature. The parameters used in the model are illustrated in Fig. 1*b, c* including: leaf base height (distance between the leaf base and the ground); leaf length (maximal length of a leaf when stretched to be straight); leaf width (maximum width of each leaf); leaf angle (angle between leaf blade and stem); and leaf curvature radius (leaf curvature along its longitudinal axis was assumed to correspond to an arc of a circle, the radius of which was termed leaf curvature radius).

Features of the canopy architecture of rice at the grain filling stage were obtained by taking average architectural parameters from three rice plants. To illustrate the procedure used to obtain average parameters, we assumed that each plant has m tillers and each tiller has n leaves. We first ordered and labelled all tillers in a plant according to its tiller height and all leaves in a tiller

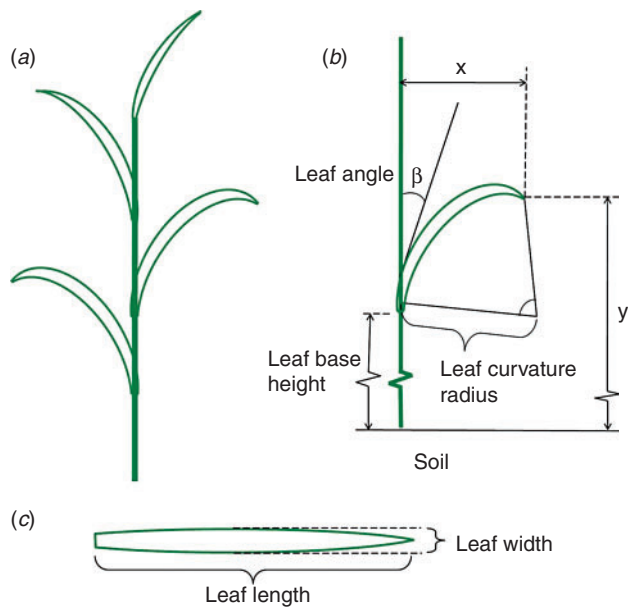


Fig. 1. (a) A single rice tiller with alternative leaf arrangement. (b) The leaf and canopy architectural features, which were used to construct the 3D canopy model in the mCanopy script (leaf angle β , leaf curvature radius and leaf base height) and (c) (leaf length and leaf width). Leaf angle is the angle between leaf base and stem: x is the horizontal distance between leaf tip and stem and y is the distance between leaf tip and ground surface. The leaf curvature radius is calculated based on x and y assuming that the leaf blade represents an arc section of a circle.

according to the leaf base heights. Then each leaf can be uniquely labelled as leaf (i, m, n), where i is the plant number (i.e. 1, or 2 or 3), m and n are the tiller number and leaf number. The average of a canopy architectural parameter is then calculated as the average value of the parameter for a leaf with the same index m and n .

A rice plant constructed with the averaged features was used to develop a canopy model (Fig. 2). Here the canopy included 64 rice plants (eight rows by eight columns) with row and column distances both being 25 cm. Each plant in the model contained 13 tillers and each tiller contained 3–5 leaves with alternate leaf arrangement (Fig. 1a). A leaf was represented as a rectangle with measured leaf width, leaf length, leaf angle and curvature, which

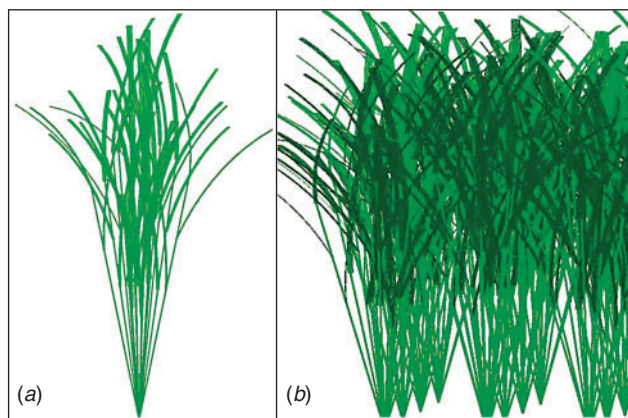


Fig. 2. (a) A 3D plant with 14 tillers and a rice canopy re-constructed with the mCanopy program.

was divided into 5-cm long segments and each segment was divided into two parts by the major vein of the leaf. The individual section of a leaf surface, defined by four edges or four points, was defined as a facet. Leaves on a tiller were arranged alternately with a random orientation angle and measured distance from leaf base to the base of the tiller. Tillers in a plant were arranged symmetrically so that taller tillers formed an inner circle and shorter tillers formed an outer circle. Many individual plants were generated individually and then combined to form a canopy. We randomly oriented each plant in the canopy. A MatLab script (MathWorks, Natick, MA, USA), mCanopy, was developed to construct the 3D model (code available from authors upon request). The canopy model can be adjusted by varying parameters of the canopy architectures.

Prediction of the light environment inside a 3D canopy with a forward ray tracing algorithm

We developed a java program (fastTracer; PICB, Shanghai, China) that uses canopy architecture model as input to simulate the light distribution inside a canopy with a forward ray tracing algorithm. The fastTracer can predict the light environment not only for a canopy with defined architecture, but also for a canopy constructed based on 3D co-ordinate data from 3D digital equipment (e.g. FASTSCAN <http://www.fastscan3d.com/>, accessed 4 December 2012).

The basic unit of a leaf surface was assumed to be facet, defined by four boundaries or points. The model is able to simulate three categories of light, i.e. direct light, diffuse light and scattered light (Fig. 3a–c). The direction of direct light is determined by the solar elevation angle, which further depends on the time and location for each particular simulation (Appendix 2, Eqn A26–29). The direction of the diffuse light is randomly distributed with equal probability in each direction. Scattered light is generated once a direct or diffuse light ray hits a leaf surface with the model of Cook-Torrance bidirectional reflectance distribution function (BRDF) (Torrance and Sparrow 1967; Cook and Torrance 1981) and Lambert bidirectional transmittance distribution function (BTDF) models (Grant 1987). The directions of scattered light were simulated with a Monte Carlo method (Tucker and Garratt 1977). The leaf absorbance is different under different incident angles (Brodersen and Vogelmann 2010). As a simplification, this model assumed an average leaf absorbance of 0.85.

A forward ray tracing algorithm simulates the path of a light ray from its source until it is finally absorbed completely by its illuminated objective. The ray tracing process in the model is shown in Fig. S1, available as Supplementary Material to this paper. In this study, a cuboid (length 1 m, width 1 m and height 2.8 m) in the centre of the reconstructed canopy, which had a length >2 m, a width >2 m and a height <2.8 m, was chosen and only leaves inside the cuboid were used in the simulation to avoid boundary effects. The light source used in the simulation is mimicked by a cluster of light ray with a density (η) of 10^6 light rays per square meter above the cuboid (Fig. 3e). The cuboid is divided into many cubes and the light is traced from one cube to another (Fig. 3e). The facets in the cube were checked to determine whether it is hit by the light ray. In our algorithm, when a light ray hits the boundary of the cuboid, this light ray is

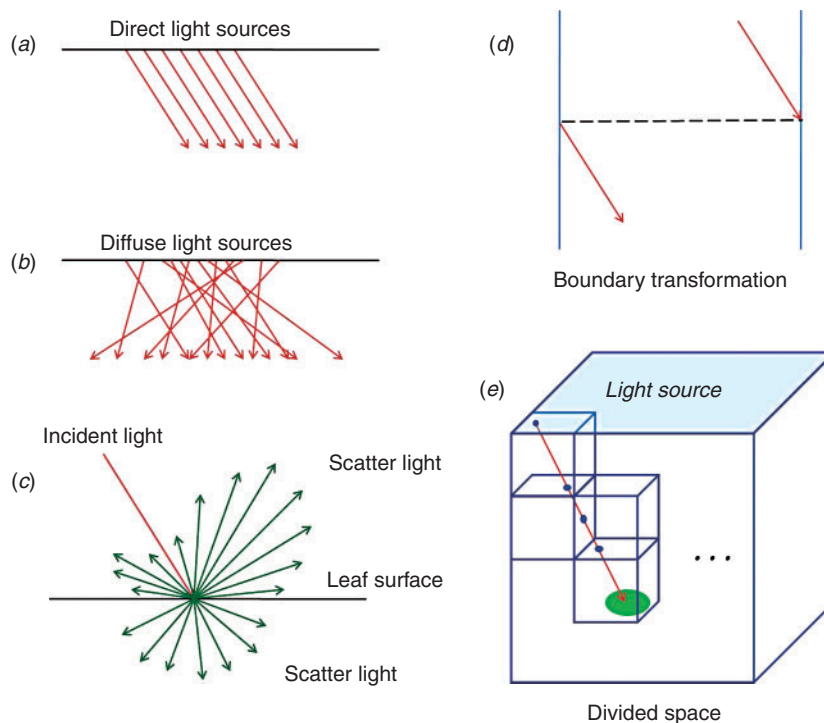


Fig. 3. Schematic representation of the ray tracing algorithm used to simulate the light distribution in a plant canopy. Direct light is represented with parallel lines (a), diffuse light with lines with random directions (b) and scattered light (c). When a light ray hits the boundary of the model geometry (a big cuboid), it was moved to a symmetrical position on the opposite side of the cuboid (d). The cuboid was divided into many cubes and light was traced from one cube to a neighbouring cube (e).

moved to the opposite side of the cuboid (Fig. 3d). For direct light, the directions of the light rays are parallel to each other; while for diffuse light, the directions of these light rays are randomised. The value of photosynthetic photon flux density (PPFD) on each facet (I_f) is calculated by dividing the absorbed light energy (e_i is the energy of each ray, N is the number of rays) intercepted by a facet with area s .

$$I_f = \frac{(e_i \times N)}{s}, \quad (1)$$

$$e_i = \frac{I}{\eta}. \quad (2)$$

Each facet ABCD (a rectangle) has four boundaries, i.e. AB, BC, CD and DA. In our forward ray tracing algorithm, the intersection point, $P(x_1, y_1, z_1)$, of the light ray with the plane ABCD is first calculated. Then, it is determined whether point P is inside ABCD or not. To do this, the rectangle ABCD is divided into two triangles ABC and ACD to check whether the point falls into ABC or ACD. If the sum of the areas of PAB, PBC and PCA equals the area of ABC (Eqn 3), point P is inside the triangle ABC.

$$S_{PAB} + S_{PBC} + S_{PCA} = S_{ABC}. \quad (3)$$

The reflected and transmitted light rays are generated once a light ray hits a leaf surface. The energy of reflected light ray (e_r) or transmitted light ray (e_t) were assumed to be 7.5% of energy of

incident light ray (e_i) and their directions were determined with a Monte Carlo method (Halton 1970) as in work by Lao *et al.* (2005).

Prediction of the macroclimatic conditions

The light environment above the canopy is influenced by atmospheric transmittance. During a growing season of a particular crop, the air transmittance varies. In this study, we assumed an atmospheric transmittance of 0.7. The directions and PPFD of direct light and diffuse light are needed to run the forward ray tracing algorithm. The PPFD of incoming solar radiation can be provided either by measured values or through prediction using mechanistic physical models. In the current study, we used a macroclimate model (Humphries and Long 1995) (Appendix 2, Eqns A22–31), which has been used in several previous studies of canopy photosynthesis e.g. (Zhu *et al.* 2004a, 2004b). Solar elevation angle, azimuth angle and PPFD of direct and diffuse light are calculated following Eqns A26–31 in Appendix 2. The predicted light environment inside the canopy using the forward ray tracing algorithm is used in (Eqns 1, 2) to predict the total canopy CO_2 uptake rate.

Calculation of the canopy photosynthesis

The photosynthetic CO_2 uptake rates (A) for each facet in a canopy is predicted by combining the steady-state biochemical model of leaf photosynthesis (Farquhar *et al.* 1980) with the predicted

PPFD. Canopy photosynthetic CO₂ uptake rate (A_c) is calculated by dividing the total photosynthetic CO₂ uptake for all the leaves above a ground area S_{ground} by the ground area.

$$A_c = \frac{\sum A_i \cdot S_i}{S_{\text{ground}}}, \quad (4)$$

The daily canopy photosynthetic CO₂ uptake rate (A'_c) is the integral of A_c during a whole day. In the calculation, A_c is numerically integrated.

$$A'_c = \int_{t=1}^{24} A_{c,t} dt = \int_{t=1}^{24} \int_{u=0}^{3600} A_c du dt \approx \sum_{t=1}^{24} A_{c,u} \times 3600, \quad (5)$$

where $A_{c,t}$ is the total photosynthetic CO₂ uptake for a unit ground area during a particular hour; $A_{c,u}$ represents the total canopy photosynthetic CO₂ uptake rate at the middle of an hour, i.e. at 30th minute of each hour.

Influence of different canopy architectural parameters on A'_c under current and future CO₂ concentrations

We examined the influences on daily total canopy CO₂ uptake by several canopy architectural parameters including stem height, leaf width and leaf angle. We further studied the effects of elevated CO₂ on the theoretically optimal canopy architectural parameters to gain maximal A_c . In the study of the influence of elevated atmospheric CO₂ concentration (C_a) on A_c , we used three scenarios: (i) current temperature (T) and current C_a of 380 μbar ; (ii) elevated temperature ($T+1.5^\circ\text{C}$) and C_a of 550 μbar , mimicking the scenario of 2050; and (iii) elevated temperature ($T+3^\circ\text{C}$) and a C_a of 760 μbar , mimicking the scenario of 2100 based on work by Parry *et al.* (2007). The temperature dependence of the parameters for leaf photosynthesis and respiration are detailed in Eqn A7–15 in Appendix 1. Following work by Davey *et al.* (2004), we assumed that dark

respiration (i.e. R_d) under elevated CO₂ is 13% higher than that under the ambient CO₂ level.

Determination of the light-limited and light saturated photosynthesis in a light response curve

In addition to label photosynthetic CO₂ uptake as limited by either RuBP-limited photosynthesis or Rubisco-limited photosynthesis following the Farquhar *et al.* (1980) model, in this work, we also label photosynthesis as either light-limited or light-saturated. To do this, we first calculated the slope of the light response curve at each light level. The point on the light response curve where the slope is 0.005 was marked as the transition point between light-limited and light-saturated photosynthesis.

Results

Fig. 4 shows PPFD of the predicted direct, diffuse and scattered light at every facet in the plant canopy. When fitting the data with Beer's Law, the coefficients of determination, R^2 , are 0.24 for direct light, 0.90 for diffuse light and 0.41 for all light. From Fig. 4c the distribution of scattered light differs from those of direct and the diffuse light in the canopy. From the top to the bottom layers of the canopy, the PPFD of scattered light first increases and then decreases. Fig. 4d shows the gradient of total PPFD with depth on every facet in the canopy.

To demonstrate the impacts of using average instead of the detailed PPFD distribution on estimating A_c , we compared the A_c calculated from average and detailed PPFDs. For this analysis, the canopy was divided into 15 layers with the height of each layer being 5.49 cm. In each layer, PPFD of all facets were averaged and then used to calculate A_c . Fig. 5 shows that A_c calculated with averaged PPFD is higher than that with the detailed PPFD at each time point, especially at midday when PPFD is high. Integrating A_c for a whole day calculated with average PPFD was 25% higher than that predicted with the detailed PPFD on each facet (Fig. 5).

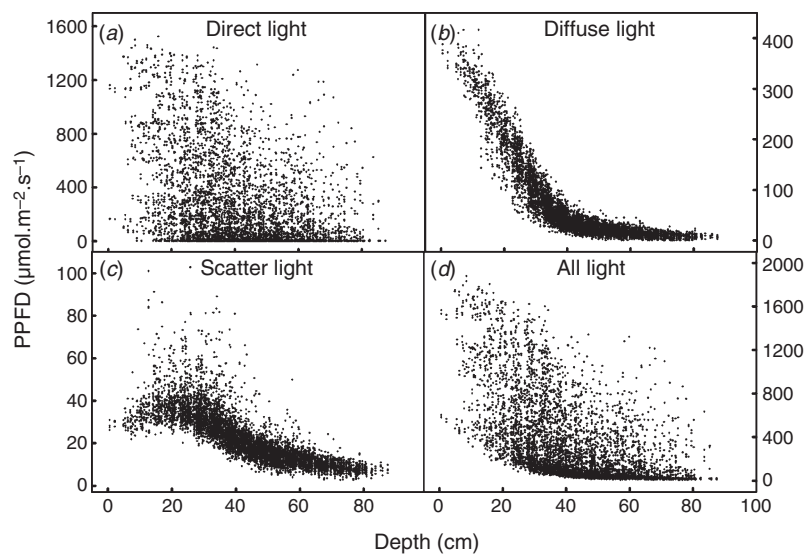


Fig. 4. Predicted distributions of direct, diffuse and scattered light at different depths of a canopy at 1130 hours on day 253 at a latitude of 39.92°N. Each point represents the photosynthetic photon flux density (PPFD) of light absorbed by a facet on a leaf in the canopy.

The leaf light response curves (Fig. 6) for the three combinations of CO₂ and temperature were predicted with the Farquhar *et al.* (1980) model with the temperature response functions of photosynthetic parameters following work by Bernacchi *et al.* (2001). Fig. 7d shows the proportion of leaf area in a canopy performing light-limited or light-saturated photosynthesis based on the scenarios (with the current air temperature and CO₂ concentration). More than 71% of the leaf area was predicted to perform light-limited photosynthesis throughout the day. At a C_a of 380 μbar, leaves performing light-limited photosynthesis absorb 32% of total incident solar energy and contributed ~47% of A_c (Fig. 7a). With an increase in C_a, the proportion of leaf area conducting light-limited photosynthesis gradually increases (Fig. 7c). Furthermore, with increasing C_a, the proportion of RuBP-limited photosynthesis forms a greater proportion of total A_c (Fig. S2). Because in the current simulation, we assumed that plants had no photosynthesis acclimation (i.e. no changes in both the maximum rate of

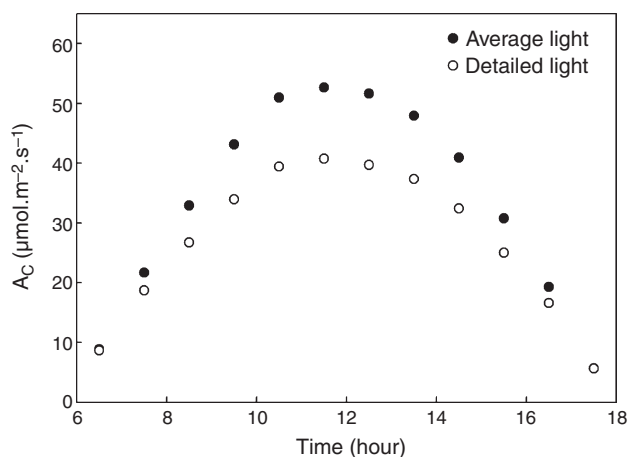


Fig. 5. The diurnal canopy CO₂ uptake rate (A_c) calculated with average photosynthetic photon flux density (PPFD) at different layers of a canopy (average light) compared with A_c calculated using the detailed PPFD of each individual facet in the canopy (detailed light).

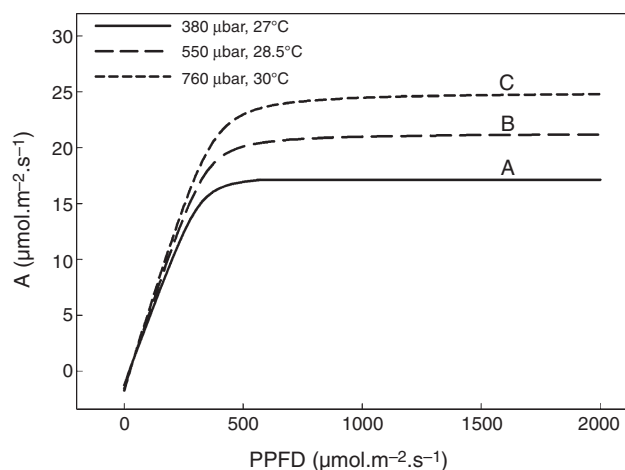


Fig. 6. The predicted light response curves under three different combinations of atmospheric CO₂ concentration (C_a) and air temperature (T_{air}).

carboxylation at RuBP and CO₂ saturation (V_{cmax}) and the light saturated potential rate of whole chain electron transport through PSII (J_{max}) under elevated CO₂, representing a scenario where plenty of nitrogen is available (Long *et al.* 2004). Under this assumption, at C_a of 550 and 700 μbar, photosynthesis is completely RuBP-limited (Fig. S2).

The PPFD of each facet inside a canopy was predicted and used to theoretically study the influences of different plant architectural features on A_c . Given that the canopy structure constructed was not symmetrical, we generated many canopies with varying leaf orientations but keep the overall canopy architectural features, e.g. stem height, leaf length, leaf width, leaf angle and leaf curvature, constant. Fig. 8 shows that A_c' was not significantly affected by an increase of the stem height of the Teqing cultivar, but A_c' gradually decreased when the stem height decreased below than 60% of the current height. Fig. 9 shows the influence of leaf angle on A_c' of two plant canopies with LAI 4.8 (Fig. 9a–c) and 7.68 (Fig. 9d–f) under different combinations of C_a and T_{air}. With an increase in leaf angle, A_c' gradually increased when the LAI was 4.8. However, A_c' gradually decreased with leaf angle when LAI was 7.68. The increase in atmospheric CO₂ concentration does not change the relationship between A_c' and leaf angle. Fig. 10 shows the influence of leaf width on A_c' . In our simulations, LAI changed proportionally with leaf width when other parameters were kept constant. Results show that the optimal leaf width was around 85% of the current leaf width under current C_a (Fig. 10).

Discussion

Crop yields are related to photosynthesis of the whole canopy instead of the photosynthetic capacities of only the top leaves

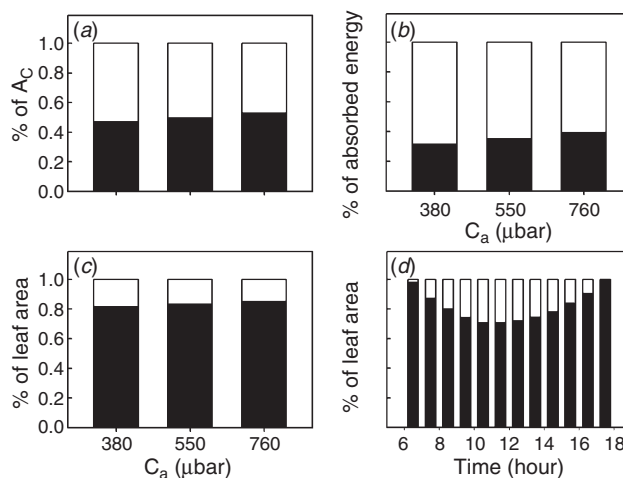


Fig. 7. The proportion of A_c contributed by light-limited photosynthesis and light-saturated photosynthesis (a); the proportion of total absorbed light energy by leaves conducting light-limited photosynthesis and light-saturated photosynthesis (b); the proportion of leaf area conducting light-limited photosynthesis and light-saturated photosynthesis (c). All these simulations were done under three CO₂ and temperature combinations. (d) The proportion of leaf area conducting light-limited or light-saturated photosynthesis at different times during a day at a CO₂ concentration of 380 μbar.

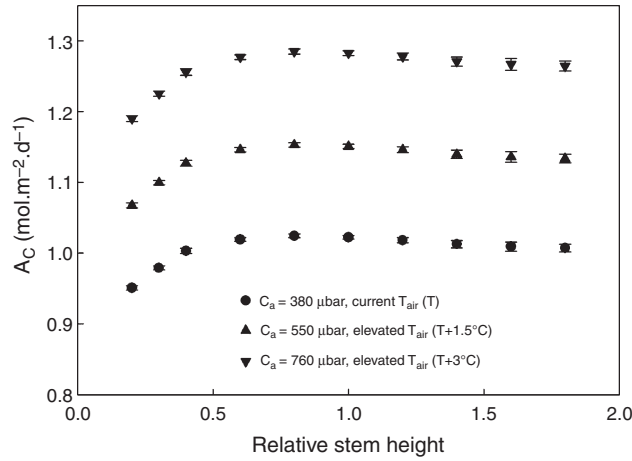


Fig. 8. The predicted influence of stem height on canopy photosynthetic CO_2 uptake rate under three different combinations of CO_2 and temperature. The points show mean \pm s.d. of nine simulations.

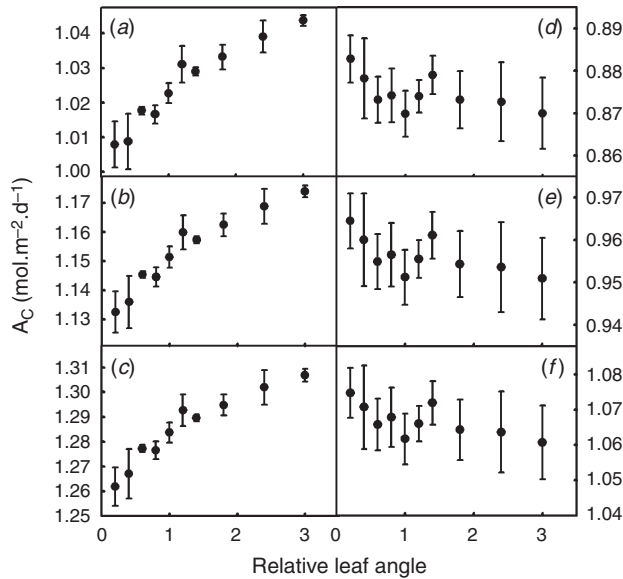


Fig. 9. The predicted influence of the leaf angle on canopy photosynthetic CO_2 uptake rate (A_c) under three different combinations of CO_2 and temperature. (a) $C_a = 380 \mu\text{bar}$, current $T_{\text{air}} (T)$; (b) $C_a = 550 \mu\text{bar}$, elevated $T_{\text{air}} (T + 1.5^\circ\text{C})$; (c) $C_a = 760 \mu\text{bar}$, elevated $T_{\text{air}} (T + 3^\circ\text{C})$; (d) $C_a = 380 \mu\text{bar}$, current $T_{\text{air}} (T)$; (e) $C_a = 550 \mu\text{bar}$, elevated $T_{\text{air}} (T + 1.5^\circ\text{C})$; (f) $C_a = 760 \mu\text{bar}$, elevated $T_{\text{air}} (T + 3^\circ\text{C})$. (a–c) $\text{LAI} = 4.8$; (d–f) $\text{LAI} = 7.68$. The points show mean \pm s.d. of nine simulations.

(Zhu *et al.* 2010, 2012). This has been demonstrated in different crops, e.g. in cotton (Wells *et al.* 1986) and soybean (Harrison and Ashley 1980). The challenge is to identify architectural and biochemical properties that can be modified to gain increased canopy photosynthetic CO_2 uptake rates. In particular, although historically canopy architecture has been a major target of breeding for most crops, it is unknown whether further improving canopy architecture will increase crop yields for current and future CO_2 conditions. The model developed here aimed to tackle this challenge through incorporation of three

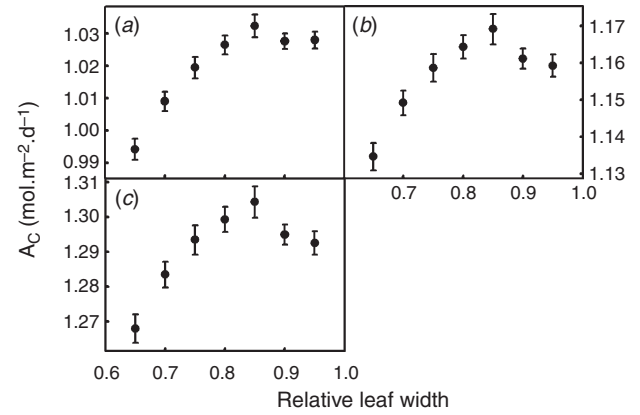


Fig. 10. The predicted influence of leaf width on canopy photosynthetic CO_2 uptake rate (A_c) under three different combinations of CO_2 and temperature. (a) $C_a = 380 \mu\text{bar}$, current $T_{\text{air}} (T)$; (b) $C_a = 550 \mu\text{bar}$, elevated $T_{\text{air}} (T + 1.5^\circ\text{C})$; (c) $C_a = 760 \mu\text{bar}$, elevated $T_{\text{air}} (T + 3^\circ\text{C})$. The points show mean \pm s.d. of nine simulations.

features. First, canopy architecture was abstracted into several properties, which enabled an easy construction of a diverse set of canopy architectures for different crops, not only crops with relatively simple architecture, e.g. maize (Fournier and Andrieu 1999), rice (Watanabe *et al.* 2005) and wheat (Fournier *et al.* 2003), but also crops with relatively complex architecture, e.g. soybean and tomato. This contrasts with previous models where canopy architecture is used as input and correspondingly cannot be easily modified (Zheng *et al.* 2008). Second, the model uses a forward ray tracing algorithm to predict the detailed PPFD of every point inside a canopy. In addition, similar to previous efforts (Lao *et al.* 2005), the transmitted and reflected light rays in this model are traced using a Monte Carlo approach (Tucker and Garratt 1977), which enables exploration of the effects of different leaf optical properties, i.e. leaf reflectance, transmittance and absorbance, on light environments inside a canopy. Third, the model combines the detailed light environment in a canopy with the steady-state biochemical model of C_3 photosynthesis (Farquhar *et al.* 1980) to simulate the daily total canopy CO_2 uptake rate (A_c). With these three features, the current model enables an accurate estimate of the impacts of different canopy architectural parameters on total canopy CO_2 uptake rate. Notably, the heterogeneous light environment inside a canopy has also been combined with the Farquhar *et al.* (1980) model in the Y-Plant system (Percy and Yang 1996; Percy and Yang 1998; Percy *et al.* 2004) and has been used to estimate the influence of different canopy features on canopy photosynthesis, revealing that leaf angle and self-shading help ameliorate photoinhibition (Percy *et al.* 2004).

With the current model, we first demonstrated that there can be a substantial difference between the estimated A_c dependent on whether the light environments on each point inside a canopy or an ‘average’ light level were used in the calculations of the photosynthetic rate. The attenuation of PPFD has been typically assumed to follow Beer’s Law (Monsi and Saeki 2005). Fig. 4b shows that PPFD of the diffuse light at different depths in a canopy is consistent with Beer’s Law ($R^2 = 0.90$), but the

distribution of direct light cannot be correctly represented by using Beer's Law. Furthermore, even if the extinction coefficient can be estimated accurately, such models can only be used to predict the average PFDs in different layers of a canopy (Ledent 1977). Because A becomes light saturated around 30% of the total PFD at solar noon, leaves receiving direct light dissipate much of its absorbed solar energy as heat (Fig. 6). This, together with the non-linearity of the response of A to PFD, results in an overestimate total CO₂ uptake for models that use an 'average' light intensity. For example, a canopy shown in this study using averaged light led to a 25% higher A_c compared with the A_c predicted with the PFD at individual points in the canopy. Though theoretically the estimated canopy photosynthetic CO₂ uptake using PFD of each point would be more accurate compared with prediction using an 'average' light level, experimental measurements of canopy photosynthetic CO₂ uptake rates using canopy chambers are needed to ultimately judge the validity of these two approaches.

The canopy photosynthesis model was used to demonstrate that photosynthetic CO₂ uptake of the shaded leaves can be more than 47% of the total A_c' . The canopy photosynthesis includes both light-limited and light-saturated photosynthesis. For the chosen LAI, V_{cmax} , J_{max} and plant architecture used in this study, more than 71% of the total leaf area conducting light-limited photosynthesis (Fig. 7d). The light-limited photosynthesis accounted for ~47% of A_c' (Fig. 7a). This demonstrates that improving photosynthesis of shaded leaves and not only that of the sunlit leaves at the top is important in terms of gaining a higher canopy photosynthetic rate. The large contribution of light-limited photosynthesis to A_c may also contribute to the lower than expected increase in A_c under elevated CO₂ (Long *et al.* 2006a). This is because when C_a is elevated to be around 550 μ bar and 760 μ bar, a higher proportion of the total leaf area will perform light-limited photosynthesis, which is less responsive to elevated CO₂ (Zhu *et al.* 2010). Some approaches to increase photosynthesis at lower layers of the canopy have been proposed recently, e.g. decreasing the leaf chlorophyll content (Ort *et al.* 2011), expanding the light spectrum (Chen and Blankenship 2011) and use Rubisco of increased specificity in the lower layer of the canopy (Zhu *et al.* 2004a; Long *et al.* 2006b).

Identification of optimal canopy architectural features can expedite ideal type breeding for higher crop yield potential (Peng *et al.* 2008; Parry *et al.* 2011). This is especially relevant given the currently increasing demand for food production (Tilman *et al.* 2011) and the recent progress in elucidating the molecular mechanisms controlling plant architecture (Wang and Li 2008). With the new mechanistic model of canopy photosynthesis, we examined the optimality of several genetically modifiable canopy architectural features, i.e. leaf width, stem height and leaf angle, for both current and future elevated CO₂ conditions. First, when leaf width and correspondingly LAI increase, the A_c' was predicted to first increase and then decrease (Fig. 10). This pattern is caused by trade-off between increased A_c and the unavoidable increase in respiratory cost under elevated LAI. The optimal leaf width for this rice cultivar is predicted to be ~85% of that in the current cultivar (Fig. 10), suggesting a potential target for genetic engineering.

With an increase in stem height, A_c was predicted to gradually increase until it plateaued (Fig. 8). This pattern held under all three CO₂ concentrations (C_a) used in this study. We note that the optimal stem height is ~80% of that of the Teqing cultivar. This indicates that even though the rice height has been dramatically decreased during the 'green revolution', there is still space for further decrease, which can potentially improve rice yields, given that decreased stem height contributes to lodging resistance and can decrease respiratory cost for building and maintaining the extra stem tissue (Gale *et al.* 1985; Evans 1996; Peng *et al.* 1999). It is worth noting that when the stem is too short, A_c will decrease because leaves with internode lengths below a minimum threshold will create higher mutual shading and decrease the total absorbed solar energy (Table A1 in Appendix 4).

Leaf angles in different rice cultivars differ dramatically (Mohanty and Gangopadhyay 1982). Under a relatively lower LAI of 4.8, under current and elevated C_a (Fig. 9a), the A_c was predicted to gradually increase with increase of leaf angle as a result of the decreased light penetrating the canopy and falling to the ground and correspondingly increased light absorbance. Under a relative higher LAI of 7.68, an increased leaf angle decreases A_c under current and elevated C_a because erect leaves improve light distribution in a canopy. The optimal leaf angle varies for canopies with different LAIs as those features are interdependent.

In this study, the canopy features, i.e. stem height, leaf length, leaf width, leaf angle and leaf curvature were independently adjusted to examine its optimal value. However, those features interact with each other. For example, tiller number influences are related to planting density (Fagade and Dedatta 1971). Planting density can also influence the red/far-red ratio, which can further modify the leaf length and width (Franklin *et al.* 2003). Thus far, molecular mechanisms underlining these inter-dependencies are still not well understood. In the current model, as a simplification, we did not include these inter-dependencies. In addition to this simplification, the model also included several other simplifications that will need to be improved in the future. These include (i) photosynthetic properties in different layers of the canopy are assumed to be the same, (ii) perturbation of leaf position by wind is ignored and (iii) the CO₂, temperature and humidity profiles in the canopy were assumed to be uniform.

Canopy microclimatic parameters, e.g. PFD, leaf temperature, CO₂ and water vapour concentrations, differ at different depths in a canopy. Furthermore, many leaf traits, e.g. chlorophyll concentration, V_{cmax} and J_{max} , also vary with leaf age and position of a leaf inside a canopy. These environmental and physiological heterogeneities can influence the estimate of A_c and correspondingly, the choice of the optimal parameter values to maximise canopy photosynthesis. For example, the assumed constant chlorophyll concentration inside a canopy might potentially under-estimate PFD in the lower layer of a canopy because chlorophyll concentration of leaves in lower layer is usually higher than that of leaves in top layer (Ciganda *et al.* 2008). Furthermore, using an average constant V_{cmax} and J_{max} values instead of using actual gradients of V_{cmax} and J_{max} values in a canopy can also potentially underestimate A_c . So far it has been a major challenge to measure these leaf physiological parameters with a throughput required to effectively parameterise a canopy

photosynthesis model. In this regard, it is encouraging that a spectroscopic method (Serbin *et al.* 2012) based on leaf reflective spectra can estimate a range of leaf physiological parameters including chlorophyll content, leaf specific area, V_{cmax} and J_{max} , with relatively high levels of accuracy.

In summary, we developed a new model of canopy photosynthesis, the aim of which was to provide a direct linkage between canopy architectural parameters with a detailed light distribution inside a canopy and correspondingly total canopy photosynthetic CO_2 uptake rate. Although several areas in the model still need to be further developed, the model already provides a useful framework for designing ideal crop architectures to optimise light distribution and enhance photosynthetic CO_2 uptake for different crops under different light and CO_2 conditions. One major challenge now is to link the model predictions with experimentally-measured canopy light environments and canopy photosynthetic CO_2 uptake rates. Only after such a close linkage is fully established can the potential of such modelling approach in guiding crop improvements be fully realised.

Acknowledgements

We thank Dr Jianlong Xu for providing the plants for the collection of canopy features. Funding for authors' research is from National Science Foundation of China (Grant No. 30970213), Ministry of Science and Technology of China (Grant Nos 2011DFA31070 and S2012GR0368), the Bill and Melinda Gates Foundation (Grant No. OPP1014417), the Young Talent Frontier Program of Shanghai Institutes for Biology Sciences/Chinese Academy of Sciences (Grant No. 2011KIP311) and EU FP7 project Grassmargins (Grant No. EU 289461).

References

- Acock B, Charles-Edwards DA, Fitter DJ, Hand DW, Ludwig LJ, Warren Wilson J, Withers AC (1978) The contribution of leaves from different levels within a tomato crop to canopy net photosynthesis: an experimental examination of two canopy models. *Journal of Experimental Botany* **29**, 815–827. doi:10.1093/jxb/29.4.815
- Amthor JS (1994) Scaling CO_2 -photosynthesis relationships from the leaf to the canopy. *Photosynthesis Research* **39**, 321–350. doi:10.1007/BF00014590
- Bernacchi CJ, Singaas EL, Pimentel C, Portis AR, Long SP (2001) Improved temperature response functions for models of Rubisco-limited photosynthesis. *Plant, Cell & Environment* **24**, 253–259. doi:10.1111/j.1365-3040.2001.00668.x
- Boote KJ, Loomis RS (1991) The prediction of canopy assimilation. In 'Modeling crop photosynthesis – from biochemistry to canopy. Special Publication No. 19'. pp. 109–140. (CSSA: Madison, WI)
- Brodersen CR, Vogelmann TC (2010) Do changes in light direction affect absorption profiles in leaves? *Functional Plant Biology* **37**, 403–412. doi:10.1071/FP09262
- Catovsky S, Holbrook NM, Bazzaz FA (2002) Coupling whole-tree transpiration and canopy photosynthesis in coniferous and broad-leaved tree species. *Canadian Journal of Forest Research* **32**, 295–309. doi:10.1139/x01-199
- Chen M, Blankenship RE (2011) Expanding the solar spectrum used by photosynthesis. *Trends in Plant Science* **16**, 427–431. doi:10.1016/j.tplants.2011.03.011
- Chen HS, Dickinson RE, Dai YJ, Zhou LM (2011) Sensitivity of simulated terrestrial carbon assimilation and canopy transpiration to different stomatal conductance and carbon assimilation schemes. *Climate Dynamics* **36**, 1037–1054. doi:10.1007/s00382-010-0741-2
- Ciganda V, Gitelson A, Schepers J (2008) Vertical profile and temporal variation of chlorophyll in maize canopy: quantitative 'crop vigor' indicator by means of reflectance-based techniques. *Agronomy Journal* **100**, 1409–1417. doi:10.2134/agronj2007.0322
- Cook R, Torrance KE (1981) A reflectance model for computer graphics. *Computer Graphics* **15**, 307–316. doi:10.1145/965161.806819
- Dai Y, Robert ED, Wang Y-P (2004) A two-big-leaf model for canopy temperature, photosynthesis, and stomatal conductance. *Journal of Climate* **17**, 2281–2299. doi:10.1175/1520-0442(2004)017<2281:ATM FCT>2.0.CO;2
- Davey PA, Hunt S, Hymus GJ, DeLucia EH, Drake BG, Karnosky DF, Long SP (2004) Respiratory oxygen uptake is not decreased by an instantaneous elevation of $[\text{CO}_2]$, but is increased with long-term growth in the field at elevated $[\text{CO}_2]$. *Plant Physiology* **134**, 520–527. doi:10.1104/pp.103.030569
- de Pury DGG, Farquhar GD (1997) Simple scaling of photosynthesis from leaves to canopies without the errors of big-leaf models. *Plant, Cell & Environment* **20**, 537–557. doi:10.1111/j.1365-3040.1997.00094.x
- deWit CT (1965) Photosynthesis of leaf canopies. Agricultural Research Report No. 663. (PUDOC: Wageningen, The Netherlands)
- Duncan WG, Loomis RS, Williams WA, Hanau R (1967) A model for simulating photosynthesis in plant communities. *Hilgardia* **38**, 181–205.
- España ML, Baret F, Aries F, Chelle M, Andrieu B, Prévot L (1999) Modeling maize canopy 3D architecture: application to reflectance simulation. *Ecological Modelling* **122**, 25–43. doi:10.1016/S0304-3800(99)00070-8
- Evans LT (1996) 'Crop evolution, adaptation and yield.' (Cambridge University Press: Cambridge)
- Evers JB, Vos J, Fournier C, Andrieu B, Chelle M, Struik PC (2007) An architectural model of spring wheat: evaluation of the effects of population density and shading on model parameterization and performance. *Ecological Modelling* **200**, 308–320. doi:10.1016/j.ecolmodel.2006.07.042
- Fagade SO, Dedatta SK (1971) Leaf area index, tillering capacity, and grain yield of tropical rice as affected by plant density and nitrogen level. *Agronomy Journal* **63**, 503–506. doi:10.2134/agronj1971.00021962006300030047x
- Farquhar GD (1989) Models of integrated photosynthesis of cells and leaves. *Philosophical Transactions of the Royal Society of London. Series B, Biological Sciences* **323**, 357–367. doi:10.1098/rstb.1989.0016
- Farquhar GD, van Caemmerer S, Berry JA (1980) A biochemical-model of photosynthetic CO_2 assimilation in leaves of C_3 species. *Planta* **149**, 78–90. doi:10.1007/BF00386231
- Fournier C, Andrieu B (1999) ADEL-maize: an L-system based model for the integration of growth processes from the organ to the canopy. Application to regulation of morphogenesis by light availability. *Agronomie* **19**, 313–327. doi:10.1051/agro:19990311
- Fournier C, Andrieu B, Ljutovac S, Saint-Jean S (2003) ADEL-wheat: a 3D architectural model of wheat development. In the 'Proceedings of plant growth modeling and applications'. pp. 54–63. (Tsinghua University Press/Springer: Beijing)
- Franklin KA, Prækelt U, Stoddart WM, Billingham OE, Halliday KJ, Whitelam GC (2003) Phytochromes B, D, and E act redundantly to control multiple physiological responses in *Arabidopsis*. *Plant Physiology* **131**, 1340–1346. doi:10.1104/pp.102.015487
- Gale MD, Youssefian S, Russell GE (1985) 'Progress in plant breeding.' (Butterworths: London)
- Goudriaan J (1977) 'Crop micrometeorology: a simulation study.' (PUDOC: Wageningen, The Netherlands)
- Grant L (1987) Diffuse and specular characteristics of leaf reflectance. *Remote Sensing of Environment* **22**, 309–322. doi:10.1016/0034-4257(87)90064-2

- Gu LH, Baldocchi D, Verma SB, Black TA, Vesala T, Falge EM, Dowty PR (2002) Advantages of diffuse radiation for terrestrial ecosystem productivity. *Journal of Geophysical Research, D, Atmospheres* **107**, 4050. doi:10.1029/2001JD001242
- Guo Y, Ma YT, Zhan ZG, Li BG, Dingkuhn M, Luquet D, De Reffye P (2006) Parameter optimization and field validation of the functional-structural model GREENLAB for maize. *Annals of Botany* **97**, 217–230. doi:10.1093/aob/mcj033
- Halton JH (1970) A retrospective and prospective survey of the Monte Carlo method. *SIAM Review* **12**, 1–63.
- Harrison SA, Ashley H (1980) Heritability of canopy-apparent photosynthesis and its relationship to seed yield in soybeans. *Crop Science* **21**, 222.
- Hirabayashi S, Kroll CN, Nowak DJ (2011) Component-based development and sensitivity analyses of an air pollutant dry deposition model. *Environmental Modelling & Software* **26**, 804–816. doi:10.1016/j.envsoft.2010.11.007
- Humphries SW, Long SP (1995) WIMOVAC – a software package for modeling the dynamics of plant leaf and canopy photosynthesis. *Computer Applications in the Biosciences* **11**, 361–371.
- Johnson IR, Thornley JHM (1984) A model of instantaneous and daily canopy photosynthesis. *Journal of Theoretical Biology* **107**, 531–545. doi:10.1016/S0022-5193(84)80131-9
- Kotchenova SY, Song XD, Shabanova NV, Potter CS, Knyazikhin Y, Myneni RB (2004) Lidar remote sensing for modeling gross primary production of deciduous forests. *Remote Sensing of Environment* **92**, 158–172. doi:10.1016/j.rse.2004.05.010
- Kull O, Jarvis PG (1995) The role of nitrogen in a simple scheme to scale-up photosynthesis from leaf to canopy. *Plant, Cell & Environment* **18**, 1174–1182. doi:10.1111/j.1365-3040.1995.tb00627.x
- Lao C, Yan T, Li B (2005) Three dimensional canopy radiation transfer model based on Monte Carlo ray tracing. PhD thesis, China Agricultural University.
- Ledent JF (1977) Calculation of extinction coefficient of incident direct solar-radiation in a plant canopy. *Oecologia Plantarum* **12**, 291–300.
- Lemon E, Stewart DW, Shawcroft RW (1971) The sun's work in a cornfield. *Science* **174**, 371–378. doi:10.1126/science.174.4007.371
- Lloyd J, Grace J, Miranda AC, Meir P, Wong SC, Miranda BS, Wright IR, Gash JHC, McIntyre J (1995) A simple calibrated model of amazon rain-forest productivity based on leaf biochemical-properties. *Plant, Cell & Environment* **18**, 1129–1145. doi:10.1111/j.1365-3040.1995.tb00624.x
- Long SP, Ainsworth EA, Rogers A, Ort DR (2004) Rising atmospheric carbon dioxide: plants face the future. *Annual Review of Plant Biology* **55**, 591–628. doi:10.1146/annurev.arplant.55.031903.141610
- Long SP, Ainsworth EA, Leakey ADB, Nosberger J, Ort DR (2006a) Food for thought: lower-than-expected crop yield stimulation with rising CO₂ concentrations. *Science* **312**, 1918–1921. doi:10.1126/science.1114722
- Long SP, Zhu XG, Naidu SL, Ort DR (2006b) Can improvement in photosynthesis increase crop yields? *Plant, Cell & Environment* **29**, 315–330. doi:10.1111/j.1365-3040.2005.01493.x
- Miguez FE, Zhu XG, Humphries S, Bollero GA, Long SP (2009) A semimechanistic model predicting the growth and production of the bioenergy crop *Miscanthus × giganteus*: description, parameterization and validation. *GCB Bioenergy* **1**, 282–296. doi:10.1111/j.1757-1707.2009.01019.x
- Mo XG, Liu SX (2001) Simulating evapotranspiration and photosynthesis of winter wheat over the growing season. *Agricultural and Forest Meteorology* **109**, 203–222. doi:10.1016/S0168-1923(01)00266-0
- Mohanty CR, Gangopadhyay S (1982) Variation of leaf angle and incidence of rice blast disease. *Journal of Agricultural Science* **98**, 225–227. doi:10.1017/S0021859600041332
- Monsi M, Saeki T (2005) On the factor light in plant communities and its importance for matter production. *Annals of Botany* **95**, 549–567. doi:10.1093/aob/mci052
- Norman JM (1979) Modeling the complete crop canopy. In 'Modification of the aerial environment of plants'. (Eds BJ Barfield, JF Gerber) pp. 249–280. (American Society Agricultural Engineers: St. Joseph, MI)
- Norman JM 1980. Interfacing leaf and canopy irradiance interception models. In 'Predicting photosynthesis for ecosystem models'. pp. 49–67. (CRC Press: Boca Raton, FL)
- Ort DR, Zhu XG, Melis A (2011) Optimizing antenna size to maximize photosynthetic efficiency. *Plant Physiology* **155**, 79–85. doi:10.1104/pp.110.165886
- Parry M, Canziani O, Palutikof J, Van der Linden P, Hanson C (2007) 'Climate change 2007: impacts, adaptation and vulnerability. Contribution of working group II to the fourth assessment report of the intergovernmental panel on climate change.' (Cambridge University Press: Cambridge)
- Parry MAJ, Reynolds M, Salvucci ME, Raines C, Andralojo PJ, Zhu XG, Price GD, Condon AG, Furbank RT (2011) Raising yield potential of wheat. II. Increasing photosynthetic capacity and efficiency. *Journal of Experimental Botany* **62**, 453–467. doi:10.1093/jxb/erq304
- Pearcy RW, Yang WM (1996) A three-dimensional crown architecture model for assessment of light capture and carbon gain by understory plants. *Oecologia* **108**, 1–12. doi:10.1007/BF00333208
- Pearcy RW, Yang W (1998) The functional morphology of light capture and carbon gain in the redwood forest understory plant *Adenocaulon bicolor* Hook. *Functional Ecology* **12**, 543–552. doi:10.1046/j.1365-2435.1998.00234.x
- Pearcy RW, Valladares F, Wright SJ, de Paulis EL (2004) A functional analysis of the crown architecture of tropical forest *Psychotria* species: do species vary in light capture efficiency and consequently in carbon gain and growth? *Oecologia* **139**, 163–177. doi:10.1007/s00442-004-1496-4
- Peng J, Richards DE, Hartley NM, Murphy GP, Devos KM, Flintham JE, Beales J, Fish LJ, Worland AJ, Pelica F, Sudhakar D, Christou P, Snape JW, Gale MD, Harberd NP (1999) 'Green revolution' genes encode mutant gibberellin response modulators. *Nature* **400**, 256–261. doi:10.1038/22307
- Peng SB, Khush GS, Virk P, Tang QY, Zou YB (2008) Progress in ideotype breeding to increase rice yield potential. *Field Crops Research* **108**, 32–38. doi:10.1016/j.fcr.2008.04.001
- Reicosky DC, Peters DB (1977) A portable chamber for rapid evapotranspiration measurements on field plots. *Agronomy Journal* **69**, 729–732.
- Reynolds JF, Chen JL, Harley PC, Hilbert DW, Dougherty RL, Tenhunen JD (1992) Modeling the effects of elevated CO₂ on plants – extrapolating leaf response to a canopy. *Agricultural and Forest Meteorology* **61**, 69–94. doi:10.1016/0168-1923(92)90026-Z
- Roderick ML, Farquhar GD, Berry SL, Noble IR (2001) On the direct effect of clouds and atmospheric particles on the productivity and structure of vegetation. *Oecologia* **129**, 21–30. doi:10.1007/s00442-0100760
- Running SW, Coughlan JC (1988) A general model of forest ecosystem processes for regional applications. I. Hydrological balance, canopy gas exchange and primary production processes. *Ecological Modelling* **42**, 125–154. doi:10.1016/0304-3800(88)90112-3
- Sellers PJ, Berry JA, Collatz GJ, Field CB, Hall FG (1992) Canopy reflectance, photosynthesis, and transpiration. 3. A reanalysis using improved leaf models and a new canopy integration scheme. *Remote Sensing of Environment* **42**, 187–216. doi:10.1016/0034-4257(92)90102-P
- Serbin SP, Dillaway DN, Kruger EL, Townsend PA (2012) Leaf optical properties reflect variation in photosynthetic metabolism and its

- sensitivity to temperature. *Journal of Experimental Botany* **63**, 489–502. doi:10.1093/jxb/err294
- Sinclair TR, Murphy CE, Knoerr KR (1976) Development and evaluation of simplified models for simulating canopy photosynthesis and transpiration. *Journal of Applied Ecology* **13**, 813–829. doi:10.2307/2402257
- Steduto P, Cetakoku O, Albrizio R, Kanber R (2002) Automated closed-system canopy-chamber for continuous field-crop monitoring of CO₂ and H₂O fluxes. *Agricultural and Forest Meteorology* **111**, 171–186. doi:10.1016/S0168-1923(02)00023-0
- Thornley JHM, Johnson IR (1990) 'Plant and crop modelling—a mathematical approach to plant and crop physiology.' (The Blackburn Press: Caldwell, NJ)
- Tilman D, Balzer C, Hill J, Befort BL (2011) Global food demand and the sustainable intensification of agriculture. *Proceedings of the National Academy of Sciences of the United States of America* **108**, 20260–20264. doi:10.1073/pnas.1116437108
- Torrance K, Sparrow EM (1967) Theory for off-specular reflection from roughened surfaces. *Journal of the Optical Society of America* **57**, 1105–1114. doi:10.1364/JOSA.57.001105
- Tucker CJ, Garratt MW (1977) Leaf optical system modeled as a stochastic process. *Applied Optics* **16**, 635–642. doi:10.1364/AO.16.000635
- Tuzet A, Perrier A, Leuning R (2003) A coupled model of stomatal conductance, photosynthesis and transpiration. *Plant, Cell & Environment* **26**, 1097–1116. doi:10.1046/j.1365-3040.2003.01035.x
- Wang YP, Leuning R (1998) A two-leaf model for canopy conductance, photosynthesis and partitioning of available energy I: model description and comparison with a multi-layered model. *Agricultural and Forest Meteorology* **91**, 89–111. doi:10.1016/S0168-1923(98)00061-6
- Wang YH, Li JY (2008) Molecular basis of plant architecture. *Annual Review of Plant Biology* **59**, 253–279. doi:10.1146/annurev-arplant.59.032607.092902
- Watanabe T, Hanan JS, Room PM, Hasegawa T, Nakagawa H, Takahashi W (2005) Rice morphogenesis and plant architecture: measurement, specification and the reconstruction of structural development by 3D architectural modelling. *Annals of Botany* **95**, 1131–1143. doi:10.1093/aob/mci136
- Wells R, Meredith WR, Williford JR (1986) Canopy photosynthesis and its relationship to plant productivity in near-isogenic cotton lines differing in leaf morphology. *Plant Physiology* **82**, 635–640. doi:10.1104/pp.82.3.635
- Yang Y, Kim SH, Timlin DJ, Fleisher DH, Quebedeaux B, Reddy VR (2009) Simulating canopy transpiration and photosynthesis of corn plants under contrasting water regimes using a coupled model. *Transactions of the ASABE* **52**, 1011–1024.
- Zelitch I (1982) The close relationship between net photosynthesis and crop yield. *Bioscience* **32**, 796–802. doi:10.2307/1308973
- Zheng BY, Shi LJ, Ma YT, Deng QY, Li BG, Guo Y (2008) Comparison of architecture among different cultivars of hybrid rice using a spatial light model based on 3D digitising. *Functional Plant Biology* **35**, 900–910. doi:10.1071/FP08060
- Zhu XG, Portis AR, Long SP (2004a) Would transformation of C₃ crop plants with foreign Rubisco increase productivity? A computational analysis extrapolating from kinetic properties to canopy photosynthesis. *Plant, Cell & Environment* **27**, 155–165. doi:10.1046/j.1365-3040.2004.01142.x
- Zhu XG, Ort DR, Whitmarsh J, Long SP (2004b) The slow reversibility of photosystem II thermal energy dissipation on transfer from high to low light may cause large losses in carbon gain by crop canopies: a theoretical analysis. *Journal of Experimental Botany* **55**, 1167–1175. doi:10.1093/jxb/erh141
- Zhu XG, Long SP, Ort DR (2010) Improving photosynthetic efficiency for greater yield. *Annual Review of Plant Biology* **61**, 235–261. doi:10.1146/annurev-arplant-042809-112206
- Zhu X-G, Song Q, Ort DR (2012) Elements of a dynamic systems model of canopy photosynthesis. *Current Opinion in Plant Biology* **15**, 237–244. doi:10.1016/j.pbi.2012.01.010

Appendix 1. Equations of leaf photosynthesis models

$$A = [1 - \Gamma^*/C_i] \cdot \min(W_c, W_j, W_p) - R_d, \quad (\text{A1})$$

$$W_c = \frac{V_{c \max} \cdot C_i}{C_i + K_c[1 + O_i/K_o]}, \quad (\text{A2})$$

$$W_j = \frac{J \cdot C_i}{4.5C_i + 10.5\Gamma^*}, \quad (\text{A3})$$

$$W_p = \frac{3 \cdot T_u}{1 - \Gamma^*/C_i}, \quad (\text{A4})$$

$$J = \frac{I_2 + J_{\max} - \sqrt{(I_2 + J_{\max})^2 - 4\Theta I_2 J_{\max}}}{2\Theta}, \quad (\text{A5})$$

$$I_2 = \frac{I \cdot (1-f)}{2}, \quad (\text{A6})$$

$$\Theta = 0.76 + 0.018T - 3.7 \times 10^{-4}T^2, \quad (\text{A7})$$

$$\Gamma^* = \exp(c_{\Gamma^*} - \Delta H_{a,\Gamma^*}/RT_k), \quad (\text{A8})$$

$$C_i = 0.7C_a \cdot [(1.6740 - 6.1294 \cdot 10^{-2}T + 1.1688 \cdot 10^{-3}T^2 - 8.8741 \cdot 10^{-6}T^3)/0.73547] \\ \text{At } 25^\circ\text{C}, C_i = 0.7C_a, \quad (\text{A9})$$

$$O_i = 210[(4.7000 \cdot 10^{-2} - 1.3087 \cdot 10^{-3}T + 2.5603 \cdot 10^{-5}T^2 - 2.1441 \cdot 10^{-7}T^3)/2.6934 \cdot 10^{-2}] \\ \text{At } 25^\circ\text{C}, O_i = O_a, \quad (\text{A10})$$

$$V_{c \max} = V_{c \max 0} \exp(c_{V_{c \max}} - \Delta H_{a,V_{c \max}}/RT_k), \quad (\text{A11})$$

$$J_{\max} = J_{\max 0} \exp(c_{J_{\max}} - \Delta H_{a,J_{\max}}/RT_k), \quad (\text{A12})$$

$$R_d = R_{d0} \exp(c_{R_d} - \Delta H_{a,R_d}/RT_k), \quad (\text{A13})$$

$$K_o = \exp(c_{K_o} - \Delta H_{a,K_o}/RT_k), \quad (\text{A14})$$

(Continued next page)

Appendix 1. (continued)

$$K_c = \exp(c_{K_c} - \Delta H_{a,K_c}/RT_k), \quad (\text{A15})$$

$$g_s = \frac{-b + \sqrt{b^2 - 4ac}}{2a} \quad (\text{A16})$$

$$a = C_s, \quad (\text{A17})$$

$$b = -(g_0 \cdot C_s + 100g_1 \cdot A - C_s \cdot g_b), \quad (\text{A18})$$

$$c = -(100g_1 \cdot A \cdot RH \cdot \frac{e_{\text{air}}}{e_{\text{leaf}}} \cdot g_b + g_0 \cdot C_s \cdot g_b), \quad (\text{A19})$$

$$C_s = C_a - \frac{A}{g_b} \cdot P, \quad (\text{A20})$$

$$C_i = C_s - \frac{A}{g_s} \cdot P. \quad (\text{A21})$$

Appendix 2. Equations used in the calculation of macroclimates

$$T_{d,\text{current}} = T_a + \Delta T_a \sin \left[2\pi \frac{(d - d_s)}{365} \right], \quad (\text{A22})$$

$$\Delta T_{d,\text{current}} = \Delta T_d + (\Delta T_{d,\text{max}} - \Delta T_d) \sin \left[2\pi \frac{(d - d_s)}{365} \right], \quad (\text{A23})$$

$$DE = \sin \left\{ 2\pi \frac{[t - (t_{\text{peak}} - 6)]}{24} \right\}, \quad (\text{A24})$$

$$T = T_{d,\text{current}} + DE \cdot \Delta T_{d,\text{current}}, \quad (\text{A25})$$

$$\delta = -23.45 \cos \left(2\pi \frac{d + 10}{365} \right), \quad (\text{A26})$$

$$h = 15(t - t_n), \quad (\text{A27})$$

$$\theta_s = \arcsin (\cos(h) \cos(\delta) \cos(\Phi) + \sin(\delta) \sin(\Phi)), \quad (\text{A28})$$

$$\varphi_s = -\arccos \left(\frac{(\sin(\delta) \cos(\Phi) - \cos(h) \cos(\delta) \sin(\Phi))}{\cos(\theta_s)} \right) - \pi, \quad (\text{A29})$$

$$I_{\text{dr}} = I_s \cdot \left(\alpha \left(\frac{1}{\sin(\theta_s)} \right) \right) \cdot \sin(\theta_s), \quad (\text{A30})$$

$$I_{\text{df}} = 0.5 I_s \cdot \left(1 - \alpha \left(\frac{1}{\sin(\theta_s)} \right) \right) \cdot \sin(\theta_s), \quad (\text{A31})$$

Appendix 3. Definition and initial value of symbols

Values in parenthesis are those used in simulations, unless stated otherwise

Term	Units	Definition
A	$\mu\text{mol m}^{-2} \text{s}^{-1}$	Photosynthetic CO_2 uptake rate
A_c	$\mu\text{mol m}^{-2} \text{s}^{-1}$	Canopy CO_2 uptake per metre square ground area per second
A'_c	$\mu\text{mol m}^{-2} \text{day}^{-1}$	Canopy CO_2 uptake per metre square ground area per day
$A_{c,t}$	$\mu\text{mol m}^{-2} \text{h}^{-1}$	Total photosynthetic CO_2 uptake for a unit ground area in a particular hour
$A_{c,u}$	$\mu\text{mol m}^{-2} \text{s}^{-1}$	Total canopy photosynthetic CO_2 uptake rate at the middle point of an hour
c	Dimensionless	Scaling constant for temperature corrections of Γ^* (19.02), V_{cmax} (26.35), J_{max} (17.57), R_d (18.72), K_o (20.3), K_c (38.05)
C_i	μbar	Intercellular CO_2 partial pressure (at 25°C , $0.7 \times C_a$)
C_a	μbar	Atmosphere CO_2 partial pressure (380)
C_s	Pa	Partial pressure of CO_2 at a leaf surface
d	Day	Day of a year
d_s	Day	Start day temperature cycle (113)
e_{air}	Pa	Partial pressure of the saturated water vapour for the air temperature (at 25°C , 3100.69)
e_{leaf}	Pa	Partial pressure of the saturated water vapour for the leaf temperature (at 25°C , 3100.69)
e_i	$\mu\text{mol s}^{-1}$	Photosynthetic photon flux that a solar ray represents
e_r, e_t	$\mu\text{mol s}^{-1}$	Photosynthetic photon flux that a reflected or transmitted solar ray represents
f	Dimensionless	Factor to correct spectral quality (0.15)
g_s	$\text{mmol m}^{-2} \text{s}^{-1}$	Stomatal conductance
g_0	$\text{mmol m}^{-2} \text{s}^{-1}$	Stomatal coefficient g_0 (20)
g_1	$\text{mmol mbar}^{-1} \text{s}^{-1}$	Stomatal coefficient g_1 (11.35)
g_b	$\text{mmol m}^{-2} \text{s}^{-1}$	Boundary conductance (1000)
ΔH_a	kJ mol^{-1}	Activation energy for the temperature correction of Γ^* (37.87), K_c (79.43), K_o (36.38), dark respiration (46.39), V_{cmax} (65.33), J_{max} (43.54)
I	$\mu\text{mol m}^{-2} \text{s}^{-1}$	PPFD of absorbed light
I_s	$\mu\text{mol m}^{-2} \text{s}^{-1}$	Solar constant (2600)
I_{dr}	$\mu\text{mol m}^{-2} \text{s}^{-1}$	PPFD of direct light
I_{df}	$\mu\text{mol m}^{-2} \text{s}^{-1}$	PPFD of diffuse light
I_f	$\mu\text{mol m}^{-2} \text{s}^{-1}$	PPFD on the surface of facet
I_2	$\mu\text{mol m}^{-2} \text{s}^{-1}$	PPFD absorbed by PSII
J	$\mu\text{mol m}^{-2} \text{s}^{-1}$	Rate of whole chain electron transport through PSII
J_{max}	$\mu\text{mol m}^{-2} \text{s}^{-1}$	Light saturated potential rate of whole chain electron transport through PSII for a given photon flux density absorbed by PSII (at 25°C , 122.05)
K_c	μbar	Rubisco Michaelis constant CO_2 (at 25°C , 404)
K_o	mbar	Rubisco Michaelis constant O_2 (at 25°C , 278)
O_a	mbar	Atmosphere O_2 partial pressure (210)
O_i	mbar	intercellular O_2 partial pressure (at 25°C , 210)
R_d	$\mu\text{mol m}^{-2} \text{s}^{-1}$	Dark respiration coefficient (1.1)
R	$\text{J mol}^{-1} \text{K}^{-1}$	Gas constant (8.314)
RH	Dimensionless	Relative humidity (0.7)
S_{ABC}	m^2	Area of triangular ABC. The same with S_{PAB} , S_{PBC} , S_{PCA}
S_{ground}	m^2	Ground area that a canopy occupies
t	Hour	Time of a day
t_n	Hour	Time of solar noon
T_{peak}	Hour	Temperature peak hour (14)
T_a	$^\circ\text{C}$	Annual mean air temperature (12.2)
$T_{\text{d,current}}$	$^\circ\text{C}$	Daily mean air temperature for current day
ΔT	$^\circ\text{C}$	Temperature difference between leaf and air
ΔT_a	$^\circ\text{C}$	Amplitude of the annual temperature change (14)
$\Delta T_{\text{d,current}}$	$^\circ\text{C}$	Amplitude of the daily temperature change for current day
ΔT_d	$^\circ\text{C}$	Average amplitude of the daily temperature change (5.7)
ΔT_{dmax}	$^\circ\text{C}$	Maximum daily temperature change (7)
T_u	$\mu\text{mol m}^{-2} \text{s}^{-1}$	Rate of triose phosphate usage (23)
T	$^\circ\text{C}$	Temperature
T_k	K	Temperature
T_{air}	$^\circ\text{C}$	Air temperature
V	Dimensionless	Unit vector presenting direction of a reflected or transmitted light ray
V_{cmax}	$\mu\text{mol m}^{-2} \text{s}^{-1}$	Maximum rate of carboxylation at RuBP and CO_2 saturation (at 25°C , 69.28)
W_c	$\mu\text{mol m}^{-2} \text{s}^{-1}$	RuBP-saturated rate of carboxylation
W_j	$\mu\text{mol m}^{-2} \text{s}^{-1}$	RuBP-limited rate of carboxylation

(Continued next page)

Appendix 3. (continued)

Term	Units	Definition
W_p	$\mu\text{mol m}^{-2} \text{s}^{-1}$	Phosphate-limit rate of carboxylation
α	Dimensionless	Atmosphere transmittance
θ_s	Degree	Solar elevation angle
φ_s	Degree	Solar azimuth angle
δ	Degree	Sun declination angle
η	m^{-2}	Solar ray density, number of light rays per square metre
$\omega_r(\theta, \varphi)$	Dimensionless	A vector presenting direction of a reflected solar ray in the facet spherical co-ordinate system
$\omega_t(\theta, \varphi)$	Dimensionless	A vector presenting direction of a transmitted solar ray in the facet spherical co-ordinate system
Γ^*	μbar	CO_2 compensation point in the absence of dark respiration (at 25°C, 42.89)
Θ	Dimensionless	Convexity factor for the nonrectangular hyperbolic response of electron transport through PSII to photon flux (0.7)
Φ	Degree	The local latitude

Appendix 4. Solar energy absorption for rice canopies with different canopy architectural features**Table A1. Absorbed solar PPFD under different stem height**

Relative stem height	Absorbed solar PPFD \pm s.d. ($\text{mol m}^{-2} \text{day}^{-1}$)
0.2	38.23 \pm 0.06
0.3	38.87 \pm 0.09
0.4	39.56 \pm 0.10
0.6	40.07 \pm 0.10
0.8	40.65 \pm 0.13
1.0	40.86 \pm 0.14
1.2	40.93 \pm 0.23
1.4	40.69 \pm 0.20
1.6	40.57 \pm 0.18
1.8	40.61 \pm 0.16

Table A2. Absorbed solar PPFD under different leaf angle

Relative leaf angle	Absorbed solar PPFD \pm s.d. ($\text{mol m}^{-2} \text{day}^{-1}$)
0.2	39.71 \pm 0.19
0.4	40.21 \pm 0.23
0.6	40.56 \pm 0.15
0.8	40.65 \pm 0.04
1.0	40.79 \pm 0.04
1.2	41.06 \pm 0.14
1.4	40.96 \pm 0.13
1.8	41.09 \pm 0.07
2.4	41.26 \pm 0.07
3.0	41.30 \pm 0.16

Table A3. Absorbed solar PPFD under different leaf width

Relative leaf width	Absorbed solar PPFD \pm s.d. ($\text{mol m}^{-2} \text{day}^{-1}$)
0.65	37.18 \pm 0.09
0.70	37.98 \pm 0.13
0.75	38.64 \pm 0.13
0.80	39.20 \pm 0.15
0.85	39.81 \pm 0.11
0.90	40.11 \pm 0.13
0.95	40.52 \pm 0.12